Amyloid-β Induces Hepatic Insulin Resistance by Activating JAK2/STAT3/SOCS-1 Signaling Pathway

Yi Zhang, Ben Zhou, Fang Zhang, Jingxia Wu, Yanan Hu, Yang Liu, and Qiwei Zhai

Epidemiological studies indicate that patients with Alzheimer's disease (AD) have an increased risk of developing type 2 diabetes mellitus (T2DM), and experimental studies suggest that AD exacerbates T2DM, but the underlying mechanism is still largely unknown. This study aims to investigate whether amyloid-β (Aβ), a key player in AD pathogenesis, contributes to the development of insulin resistance, as well as the underlying mechanism. We find that plasma Aβ40/42 levels are increased in patients with hyperglycemia. APPswe/PSEN1dE9 transgenic AD model mice with increased plasma Aβ40/42 levels show impaired glucose and insulin tolerance and hyperinsulinemia. Furthermore, Aβ impairs insulin signaling in mouse liver and cultured hepatocytes. Aβ can upregulate suppressors of cytokine signaling (SOCS)-1, a well-known insulin signaling inhibitor. Knockdown of SOCS-1 alleviates Aβ-induced impairment of insulin signaling. Moreover, JAK2/STAT3 is activated by Aβ, and inhibition of JAK2/STAT3 signaling attenuates Aβ-induced upregulation of SOCS-1 and insulin resistance in hepatocytes. Our results demonstrate that Aβ induces hepatic insulin resistance by activating JAK2/STAT3/SOCS-1 signaling pathway and have implications toward resolving insulin resistance and T2DM. *Diabetes* **61:1434–1443, 2012**

Insulin resistance is a fundamental aspect of the etiology of type 2 diabetes mellitus (T2DM), characterized by the function of impaired insulin on glucose disposal in skeletal muscle, adipocytes, and hepatic glucose production (1). Epidemiological studies indicate patients with Alzheimer's disease (AD) have impaired glucose regulation and an increased risk of developing T2DM (2,3). Similarly, experimental studies demonstrate that the cross-bred mice of APP23 transgenic AD model mice and *ob/ob* mice showed an accelerated diabetic phenotype compared with *ob/ob* mice, which suggests that AD exacerbates T2DM (4). However, the underlying mechanism is still largely unknown.

As a normal product during cell metabolism, Aβ has an early and vital role in the pathogenesis of AD according to the amyloid cascade hypothesis (5,6). In the central nervous system, Aβ has been reported to impair neuronal synaptic function in early AD by compromising insulin signaling (7–10). On the other hand, insulin can affect both the production and degradation of Aβ (11,12). It is believed that Aβ is expressed primarily in the central nervous system, and

there is a normal dynamic equilibrium between cerebrospinal fluid and plasma Aβ (13,14). Meanwhile Aβ is also produced by peripheral cells (15,16), and peripheral tissues might contribute to both the circulating amyloid pool and AD pathology (15). But the role of Aβ in peripheral tissues is still unclear. Recent studies show that plasma Aβ levels have a positive correlation with body fat in healthy individuals and adipocyte amyloid precursor protein expression in obese individuals (17,18). These findings and the strong link between AD and T2DM (2–4) prompt us to examine whether the pathogenic factor Aβ of AD could influence insulin sensitivity in peripheral tissues.

In this study, we found that plasma Aβ40/42 levels were increased in patients with hyperglycemia. Remarkably, APPswe/PSEN1dE9 transgenic AD model mice with increased plasma Aβ40/42 levels showed impaired glucose and insulin tolerance, hyperinsulinemia, and Aβ decreased insulin sensitivity in mouse liver and cultured hepatocytes. Furthermore, we showed that Aβ impaired hepatic insulin signaling mainly through the JAK2/STAT3/suppressors of cytokine signaling (SOCS)-1 pathway.

RESEARCH DESIGN AND METHODS

Reagents. Aβ25–35, AG490, DAPI, trypan blue solution, 3-[4,5-dimethylthiazol-2-yl]-2,5-diphenyl-tetrazoliumbromide (MTT), and periodic acid Schiff (PAS) were from Sigma. Aβ42 was from Apeptide (Jiangsu, China). Aβ25–35 was dissolved in PBS at 1 mmol/L, aliquoted and stored at −80°C, and incubated at 37°C for 1 day before use as described previously (19). Aβ42 was dissolved in water at 2 mmol/L, aliquoted and stored at −80°C, and incubated at 37°C for 3 days before use as described (20). Antibodies against insulin receptor (InsR), Tyr1150/1151-phosphorylated InsR, Tyr1146-phosphorylated InsR, Thr308-phosphorylated Akt, Ser473-phosphorylated Akt, Akt, Ser9-phosphorylated glycogen synthase kinase (GSK)-3β, GSK-3β, SOCS-1, SOCS-3, Tyr705-phosphorylated STAT3, Tyr1007/1008-phosphorylated JAK2, Tyr701-phosphorylated STAT1, STAT3, or JAK2 were from Cell Signaling. Antibodies against α-tubulin or β-actin were from Sigma.

Animals. All animals were maintained and used in accordance with the guidelines of the Institutional Animal Care and Use Committee of the Institute for Nutritional Sciences. C57BL/6 mice were from Slac (Shanghai, China). APPswe/PSEN1dE9 (APP/PS1) mice and their wild-type littermates were from Jackson Laboratory (Stock number: 004462). Because the menstrual cycle could affect insulin sensitivity (21), only male mice were used in this study. The liver samples of APPswe/PS1[(A246E)] mice (Jackson Laboratory; Stock number: 003378) and the wild-type controls were provided by Dr. Weidong Le (Baylor College of Medicine). Tissues of interest were snap-frozen in liquid nitrogen immediately after resection and stored at −80°C.

Cell culture and treatments. Primary mouse hepatocytes were isolated and cultured after perfusion and collagenase digestion of the liver (22). H4IIE and HepG2 hepatoma cells were cultured in minimum essential medium and Dulbecco's modified Eagle's medium, respectively, with 10% FBS. After overnight culture, cells were treated with Aβ in serum-free medium. AG490 was added after treatment with Aβ for 24 h.

Immunoblot and ELISA. Immunoblot was performed with antibodies against the indicated protein and quantified as described (23). Plasma Aβ40/42 levels were measured by ELISA kits from Covance.

Hepatocyte glucose production. Glucose production in H4IIE cells was measured as described previously (24). In brief, after the indicated treatments, cells in 12-well plate were incubated with 300 μL per well of glucose production buffer (glucose-free Dulbecco's modified Eagle's medium, pH 7.4, containing 20 mmol/L sodium lactate and 2 mmol/L sodium pyruvate without phenol red) for

3 h at 37°C. Subsequently, 50 μL of the buffer were used to measure the glucose concentration with Glucose Assay Kit (Invitrogen), and the protein concentration of cell lysates was measured by BCA assay kit (Thermo) to normalize glucose production.

Human study. The fasting plasma of age- and sex-matched euglycemic and hyperglycemic subjects were collected in the Centre Hospital of Xuhui District, Shanghai. Patients with hyperglycemia included patients with impaired fasting glucose or diabetes as described previously (1). Patients with hypercholesterolemia were excluded. Written informed consent was obtained from each subject, and this study was approved by the Institutional Review Board of the Institute for Nutritional Sciences.

Metabolic parameters measurements. Glucose tolerance tests were performed on mice fasted for 14 h, and insulin tolerance tests were performed on mice fasted for 4 h. After fasting, the mice were injected with either 2 g/kg body weight of glucose or 0.75 units/kg body weight of human insulin (Lilly) intraperitoneally. Glucose levels were measured from tail blood using the FreeStyle blood glucose monitoring system (TheraSense) at the indicated time points. Total body fat content and lean content of mice were measured by nuclear magnetic resonance as described (23). Plasma insulin levels were measured by a radioimmunoassay kit (Beijing North Institute of Biological Technology, China). Lipid content, alanine transaminase, and aspartate transaminase activity in plasma were determined by assay kits from Sysmex.

Insulin signaling in mouse liver. After fasting for 16 h, mice were anesthetized and then injected with PBS or human insulin (2 units/kg) through their inferior vena cava. Liver samples were collected 5 min after injection.

Quantitative RT-PCR. Total RNA was isolated, treated with DNase I, and then reverse transcribed for quantitative PCR with SYBR Green using an ABI 7900 thermocycler. Relative mRNA expression was normalized to actin levels. The following primers selected from PrimerBank (http://pga.mgh.harvard.edu/primerbank/) were used: SOCS-1, CTGCGGCTTCTATTGGGGAC, AAAAGGCAGTCGAAGG-TCTCG; SOCS-3, ATGGTCACCCACAGCAAGTTT, TCCAGTAGAATCCGCTC-TCCT; actin, TGTCCACCTTCCAGCAGATGT, AGCTCAGTAACAGTCCGCCT-AGA; IL-1α, CGAAGACTACAGTTCTGCCATT, GACGTTTCAGAGGTTCTCAG-AG; IL-1β, GCAACTGTTCCTGAACTCAACT, ATCTTTTGGGGTCCGTCAACT; IL-6, TAGTCCTTCCTACCCCAATTTCC, TTGGTCCTTAGCCACTCCTTC; TNF-α, CCCTCACACTCAGATCATCTTCT, GCTACGACGTGGGCTACAG; IL-1R1, GTGC-TACTGGGGCTCATTTGT, GGAGTAAGAGGACATTTGCGAAT; IL-6R, CCTGAG-ACTCAAGCAGAAATGG, AGAAGGAAGGTCGGCTTCAGT; GP-130, CCGTGTGG-TTACATCTACCCT, CGTGGTTCTGTTGATGACAGTG; IL-8R, AACCAACAGGCA-GGCTTTAGT, CATGACGGATCGGGTCCTTC; and STAT3, CAATACCATTGACC-TGCCGAT, GAGCGACTCAAACTGCCCT.

Cell transfection and short interfering RNA. Mouse primary hepatocytes were transfected using Lipofectamine 2000 (Invitrogen). After transfection with the indicated short interfering RNA (siRNA) for 48 h, the cells were treated with Aβ in serum-free medium for 60 h. SOCS-1 siRNAs were self-designed, and STAT3 and JAK2 siRNAs were synthesized as described (25). The sense sequences of the siRNAs were as following: scrambled siRNA, uucuccgaacgugucacgu; SOCS-1 siRNA 1, ccagguggcagccgacaau; SOCS-1 siRNA 2, gagaccuucgacugccuuu; STAT3 siRNA 1, uaucaucgaccuugugaaa; STAT3 siRNA 2, ccaacgaccugcagcaaua; JAK2 siRNA 1, gcaaaccaggaaugcucaa; and JAK2 siRNA 2, ggaauggccugccuuacaa.

Immunofluorescence. Liver fresh-frozen sections of 9-month-old APPswe/PS1(A246E) mice were incubated overnight at 4°C with anti-SOCS-1 antibody, then detected with Alexa Fluor 555 goat anti-rabbit IgG. DAPI was used to stain the nuclei.

MTT assay, PAS staining, and Trypan blue staining. MTT assay was performed as described (26), and the crystals were dissolved by DMSO. PAS staining and trypan blue staining were performed following the manufacturer's instructions.

Statistical analyses. Data are expressed as mean ± S.E.M. of at least three independent experiments. Statistical significance was assessed by two-tailed unpaired Student t test. Differences were considered statistically significant at $P < 0.05$.

RESULTS

Plasma levels of Aβ correlate with hyperglycemia in humans and insulin resistance in AD mouse model. To study whether peripheral Aβ is correlated with hyperglycemia, we measured Aβ levels in human plasma. Consistent with a previous report that serum Aβ autoantibody is dramatically elevated in patients with T2DM (27), we found that both Aβ40 and Aβ42 levels were significantly increased in hyperglycemic subjects compared with age- and sex-matched euglycemic subjects (Fig. 1A and Supplementary Table 1). Because plasma Aβ levels are correlated with hyperglycemia, we hypothesized that Aβ might induce insulin resistance and hyperglycemia in vivo.

We then evaluated the potential roles of Aβ in whole-body insulin action and glucose metabolism using APPswe/PSEN1dE9 (APP/PS1) mice. The APP/PS1 double transgenic mouse is a common AD mouse model, which overexpresses amyloid precursor protein and γ-secretase leading to overexpression of Aβ40/42 and development of amyloid deposits in the brain at ~6 months of age (28). As described previously (29), we also found that plasma Aβ40/42 levels were markedly elevated in 20-week-old APP/PS1 mice before the deposit appeared (Fig. 1B). Body weight and food intake were similar between APP/PS1 and wild-type littermates (Supplementary Fig. 1A and B). Consistently, their fat content, lean content, plasma alanine transaminase and aspartate transaminase activity, and plasma triglyceride, total cholesterol, high-density lipoprotein cholesterol, and low-density lipoprotein cholesterol levels were indistinguishable with their wild-type littermates (Supplementary Fig. 1C–F). Nevertheless, the glucose tolerance tests revealed that the glucose metabolism had a significant difference at 10 weeks of age and markedly deteriorated at 18 weeks of age in APP/PS1 mice (Fig. 1C–E). The insulin tolerance tests showed that insulin sensitivity moderately decreased at 13 weeks of age and severely decreased at 19 weeks of age in APP/PS1 mice (Fig. 1F–H). Moreover, the fasting and fed plasma insulin levels were significantly increased in 20-week-old APP/PS1 mice compared with wild-type littermates (Fig. 1I), which suggests that insulin resistance induced compensatory insulin secretion in APP/PS1 mice. Taken together, these results demonstrate that APP/PS1 transgenic mice with increased plasma Aβ levels develop systemic insulin resistance.

Aβ decreases insulin sensitivity in mouse liver and cultured hepatocytes. As circulating peripheral Aβ is uptaken and catabolized mainly by liver (30), we investigate the effect of Aβ on hepatic insulin sensitivity. Immunoblot showed that insulin-stimulated phosphorylation of InsR at Tyr1150/1151, as well as Akt at Thr308 and Ser473, was markedly decreased in the liver of APP/PS1 mice (Fig. 2A and B). To explore whether Aβ can impair insulin signaling directly, we treated mouse primary hepatocytes with Aβ25–35, the biologically active fragment of Aβ (31), at the similar concentration for neuronal cells (26). Immunoblot showed that insulin-stimulated phosphorylation of InsR at Tyr1150/1151 and Tyr1146, as well as Akt at Thr308 and Ser473, and GSK-3β at Ser9 was impaired by Aβ25–35 in a dose- and time-dependent manner (Fig. 2C and D). Similarly, Aβ25–35 inhibited insulin-stimulated phosphorylation of InsR, Akt, and GSK3β in a dose- and time-dependent manner in HepG2 human hepatoma cells (Supplementary Fig. 2A and B). Full-length Aβ42 also showed similar effect on insulin signaling (Fig. 2E). We then investigated the effect of Aβ on insulin-induced suppression of glucose production in H4IIE rat hepatoma cells. Glucose release from the H4IIE cells was inhibited about 60% after insulin treatment, but the inhibitory effect of insulin on glucose output gradually declined with increasing dose of Aβ25–35 (Fig. 2F). In addition, no obvious effect of Aβ25–35 and Aβ42 on cell morphology or cell viability was observed in the above treatments, when monitored under a microscope or by MTT cell viability assay (Supplementary Fig. 3). These data demonstrate that Aβ can decrease insulin sensitivity in mouse liver and cultured hepatocytes.

Aβ induces insulin resistance in hepatocytes by upregulation of SOCS-1. It is well known that Aβ can trigger inflammatory reactions in microglia and neuron, and inflammatory signaling is involved in the development
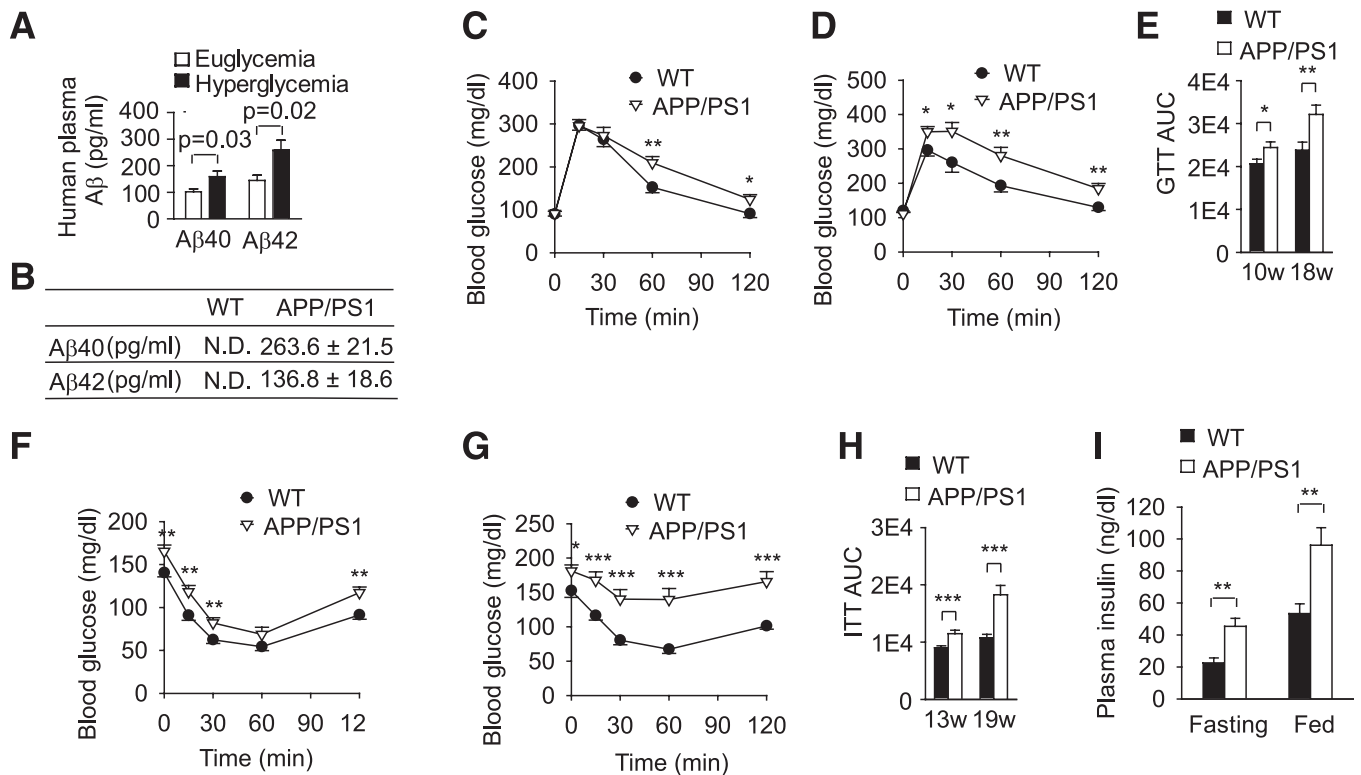
FIG. 1. Aβ affects the development of insulin resistance in vivo. *A*: Quantification of plasma Aβ40/42 levels in euglycemic and hyperglycemic subjects (*n* = 26–35 per group) by ELISA. *B*: Quantification of plasma Aβ40/42 levels in APP/PS1 mice and wild-type (WT) littermates (*n* = 4 per genotype) at 20 weeks of age by ELISA. ND, not detectable. *C* and *D*: Glucose tolerance tests (2 g/kg) in male APP/PS1 mice at the age of 10 weeks (10w; *C*) or 18 weeks (18w; *D*) (*n* = 14–16 per age) and male WT littermates (*n* = 17–19 per age). *E*: Area under the curve (AUC) of glucose tolerance tests in *C* and *D*. *F* and *G*: Insulin tolerance tests (0.75 units/kg) in male APP/PS1 mice at the age of 13 weeks (13w; *F*) or 19 weeks (19w; *G*) (*n* = 16 per age) and male WT littermates (*n* = 17–20 per age). *H*: AUC of insulin tolerance tests in *F* and *G*. *I*: Plasma insulin levels in APP/PS1 mice (*n* = 6, 4) and WT littermates (*n* = 6, 6) at 20 weeks of age under fasting and fed states. Data are presented as mean and SEM. *$P < 0.05$, **$P < 0.01$, ***$P < 0.001$.

of insulin resistance (32,33). To study whether inflammatory reactions are involved in Aβ-induced insulin resistance, we measured the inflammatory signaling in liver, muscle, and white adipose tissue (WAT) of APP/PS1 mice. We found that SOCS-1 and SOCS-3 mRNA levels were upregulated in liver (Fig. 3*A*), and the mRNA levels of GP130 in liver, IL-1α, and IL-8R in WAT were also increased (Supplementary Fig. 4*B* and *D*). However, the mRNA levels of other inflammatory factors and their downstream mediators were not altered in liver, muscle, and WAT (Supplementary Fig. 4*A*–*D*). These data suggest there was no obvious inflammatory reaction in liver, muscle, and WAT of APP/PS1 mice. It has been reported that upregulation of SOCS-1 and SOCS-3 not only inhibits cytokine signaling, but also induces insulin resistance (34,35). Immunoblot showed that the protein level of SOCS-1, but not SOCS-3, was markedly elevated in liver of APP/PS1 mice (Fig. 3*B* and *C*). To further confirm the upregulation of SOCS-1 in vivo, we measured the SOCS-1 protein level in liver of another AD mouse model, APPswe/PS1[(A246E)] transgenic mice (36). APPswe/PS1[(A246E)] mice also overexpress Aβ, and their serum Aβ42 level is about five times higher than that of APP/PS1 mice at the age of 5 months (36). Immunofluorescence showed that SOCS-1 was also elevated in liver of APPswe/PS1[(A246E)] mice (Fig. 3*D*). Taken together, these results raise the possibility that SOCS-1 might be involved in the development of insulin resistance in APP/PS1 mice.

To investigate whether the upregulation of SOCS-1 is directly induced by Aβ, we treated mouse primary hepatocytes

with Aβ25–35 and found that the mRNA level of SOCS-1, but not SOCS-3, was induced by Aβ25–35 in a time-dependent manner (Fig. 4*A*). Consistently, the SOCS-1 protein level was upregulated by Aβ25–35 in a time- and dose-dependent manner, whereas the SOCS-3 protein level remained unchanged (Fig. 4*B* and *C*). Similar results were observed when treated with Aβ42 (Fig. 4*D*). These results demonstrate that Aβ can upregulate the mRNA and protein level of SOCS-1.

To investigate whether SOCS-1 upregulation contributes to the insulin resistance induced by Aβ, we knocked down SOCS-1 by siRNA (Fig. 5*A* and *B*). As expected, knockdown of SOCS-1 by two different siRNAs all abolished the decreased phosphorylation of InsR and Akt induced by Aβ25–35 in mouse primary hepatocytes (Fig. 5*C* and *D*). Consistently, knockdown of SOCS-1 also attenuated the decreased phosphorylation of InsR and Akt induced by Aβ42 in mouse primary hepatocytes (Fig. 5*E* and *F*). These results together demonstrate that Aβ induces insulin resistance by upregulation of SOCS-1.

Aβ upregulates SOCS-1 and impairs insulin signaling in hepatocytes mainly through the JAK2/STAT3 pathway.
We next explored the mechanism by which Aβ upregulates SOCS-1. The expression of SOCS-1 can be induced by activation of the JAK/STAT pathway (34), and Aβ can regulate STAT3 and JAK2 in neurons (26,37). So we first assessed whether STAT3 can be activated by Aβ in mouse primary hepatocytes. Immunoblot showed Aβ25–35 induced phosphorylation of STAT3 at Tyr705 in a dose-dependent
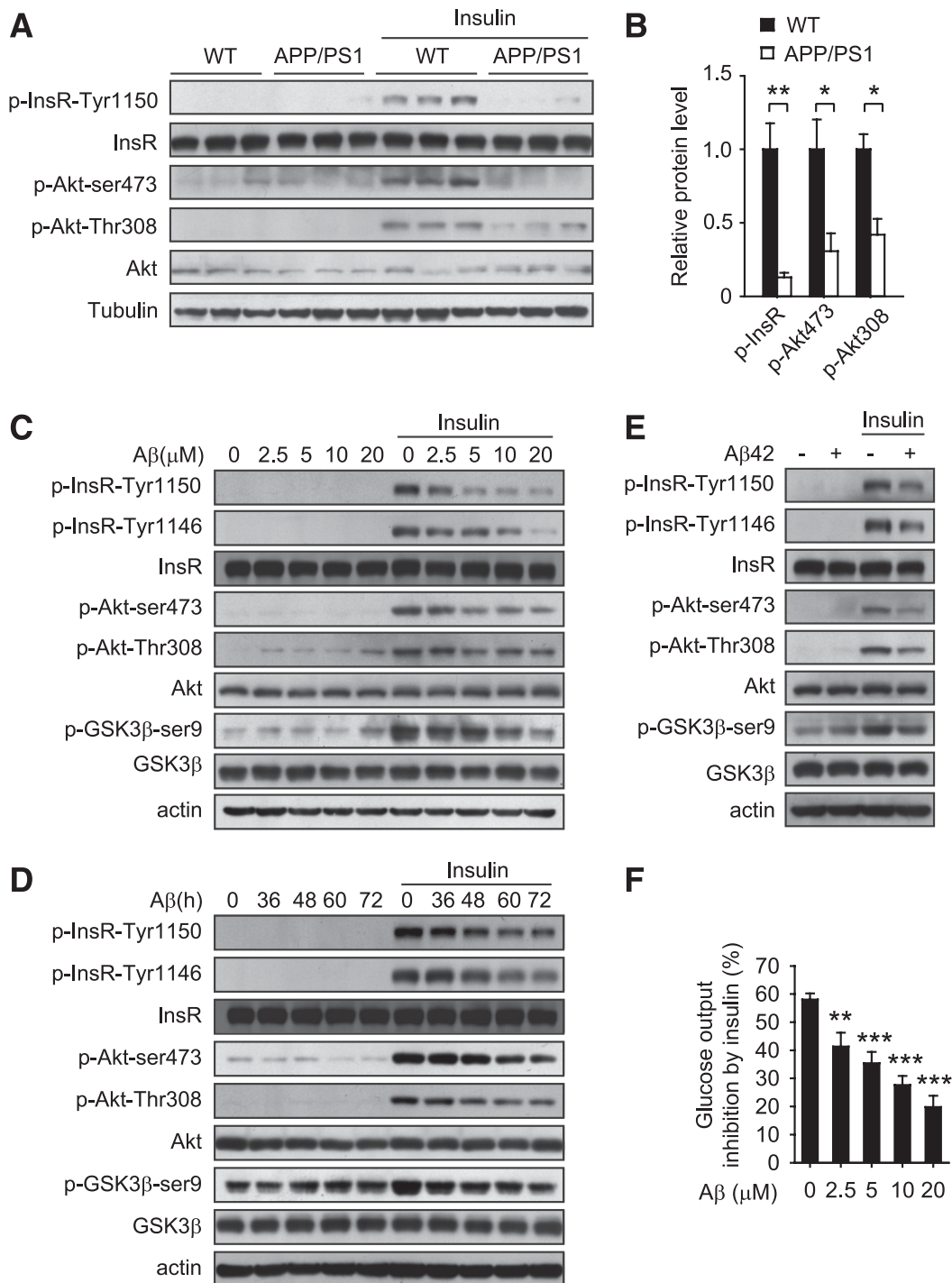
FIG. 2. Aβ impairs insulin signaling in vivo and in vitro. *A*: Insulin-stimulated phosphorylation of insulin receptor (InsR) and Akt in liver of APP/PS1 and wild-type (WT) littermates at 20 weeks of age was measured by immunoblot. *B*: Quantification of phosphorylated InsR and Akt levels in *A*. The protein levels were normalized to tubulin. *C–E*: The effect of Aβ25–35 (*C* and *D*) and Aβ42 (*E*) on insulin signaling, including the phosphorylation of InsR, Akt, and GSK-3β in mouse primary hepatocytes was analyzed by immunoblot. Cells were incubated with the indicated concentrations of Aβ25–35 for 60 h (*C*), with 10 μmol/L Aβ25–35 for the indicated times (*D*) or with 10 μmol/L Aβ42 for 60 h (*E*) followed by treatment with or without 100 nmol/L insulin for 20 min. *F*: Aβ25–35 attenuated insulin-inhibited glucose production in H4IIE rat hepatoma cells. Cells were incubated with the indicated concentrations of Aβ25–35 for 60 h and then treated with 50 nmol/L insulin for 3 h to measure the glucose production. Data are presented as mean and SEM. *$P < 0.05$, **$P < 0.01$, ***$P < 0.001$.

manner in hepatocytes, whereas phosphorylation of STAT1 at Tyr701 was not affected (Fig. 6*A*), suggesting that Aβ can specifically activate STAT3. Meanwhile phosphorylation of JAK2 at Tyr1007/1008 showed a similar pattern as STAT3 (Fig. 6*A*). Immunoblot also showed Aβ25–35 activated

STAT3 and JAK2 in a time-dependent manner in hepatocytes (Fig. 6*B*), and Aβ42 had a similar effect (Fig. 6*C*). Furthermore, we found that the tyrosine phosphorylation levels of STAT3 and JAK2 were also significantly increased in the liver of APP/PS1 mice compared with wild-type
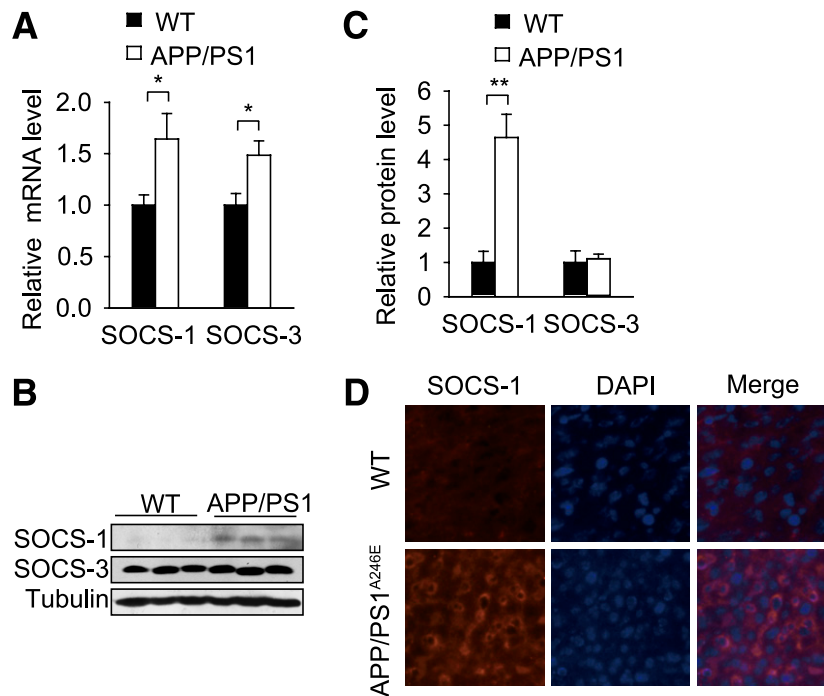
FIG. 3. Hepatic SOCS-1 is upregulated in AD mouse models. *A*: Quantitative RT-PCR analysis of liver SOCS-1 and SOCS-3 mRNA levels in APP/PS1 mice and wild-type (WT) littermates at 20 weeks of age ($n = 4$ per genotype). *B*: Immunoblot analysis of liver SOCS-1 and SOCS-3 protein levels in APP/PS1 mice and WT littermates at 20 weeks of age ($n = 3$ per genotype). *C*: Quantification of SOCS-1 and SOCS-3 protein levels in *B*. The protein levels were normalized to tubulin. *D*: Immunofluorescence analysis of liver SOCS-1 protein expression level in APPswe/PS1[(A246E)] mice and WT controls at 9 months of age. Data are presented as mean and SEM. *$P < 0.05$, **$P < 0.01$. (A high-quality digital representation of this figure is available in the online issue.)

littermates (Fig. 6*D* and *E*), suggesting JAK2/STAT3 is in a more active state in the liver of APP/PS1 mice. Immunoblot showed that the tyrosine phosphorylation levels of STAT3 and JAK2 were also elevated in the liver of APPswe/PS1[(A246E)] mice (Fig. 6*F* and *G*). These results demonstrate hepatic JAK2/STAT3 is in a more active state in mice with overexpression of Aβ.

We then determined whether SOCS-1 upregulation induced by Aβ depended on STAT3 and JAK2. Immunoblot showed that the upregulation of SOCS-1 induced by Aβ25–35 was abolished when STAT3 was knocked down by siRNA in mouse primary hepatocytes (Fig. 7*A*). Consistently, immunoblot showed that the tyrosine phosphorylation of JAK2 and STAT3 and upregulation of SOCS-1 induced by Aβ25–35 were attenuated by AG490, an inhibitor of JAK2, in hepatocytes (Fig. 7*B*). To further confirm the role of JAK2 in SOCS-1 upregulation, JAK2 was knocked down by siRNA. Similarly, immunoblot showed that tyrosine phosphorylation of JAK2 and STAT3 and upregulation of SOCS-1 induced by Aβ25–35 were attenuated when JAK2 was knocked down (Fig. 7*C* and *D*).

Next, we investigated the effect of Aβ on insulin signaling when JAK2/STAT3 signaling was inhibited. As shown in Fig. 8*A* and *B*, the decreased phosphorylation of InsR and Akt caused by Aβ25–35 was restored by STAT3 siRNA. Consistently, the decreased phosphorylation of InsR and Akt caused by Aβ25–35 was also alleviated by JAK2 inhibitor AG490 (Fig. 8*C* and *D*). Moreover, the decreased phosphorylation of InsR and Akt caused by Aβ25–35 was also alleviated by JAK2 siRNA (Fig. 8*E* and *F*). Together, these results demonstrate that Aβ activates JAK2/STAT3, which leads to SOCS-1 upregulation and insulin resistance.

DISCUSSION

The results presented here indicate that Aβ induces insulin resistance in hepatocytes by activating JAK2/STAT3/SOCS-1 signaling pathway and suggest an important role of peripheral Aβ in modulating systemic insulin sensitivity and glucose metabolism.

Although epidemiological studies indicate patients with AD have impaired glucose regulation and an increased risk of developing T2DM (2,3), only a small portion of AD patients develop impaired fasting glucose and T2DM. Notably, plasma Aβ levels in AD patients have been reported to be increased or unchanged compared with controls (38,39), which limits the utility of plasma Aβ as a diagnostic marker of AD. The marginal change of plasma Aβ in AD may at least partially explain why only a small portion of AD patients develop impaired fasting glucose and T2DM. On the other hand, epidemiological studies indicate patients with T2DM have a significantly higher risk of developing AD (40), and experimental studies suggest that T2DM exacerbates AD (41). We observed that plasma Aβ levels are elevated in hyperglycemic subjects (Fig. 1*A*), but the causality and underlying mechanism between hyperglycemia and the increased plasma Aβ levels are still unclear. It has been reported that Aβ generation or aggregation is enhanced in brain of hyperglycemic or hyperinsulinemic mice (41,42). In this study, we used APP/PS1 transgenic mice with increased plasma Aβ levels to study the potential effect of Aβ on insulin sensitivity in vivo. However, this transgenic mouse model has its limitations, and further in vivo studies would be necessary to verify the effect of Aβ on insulin signaling in peripheral tissues. Nevertheless, previous epidemiological and experimental studies combined with our findings suggest that Aβ is an important pathogenic link between T2DM and AD.
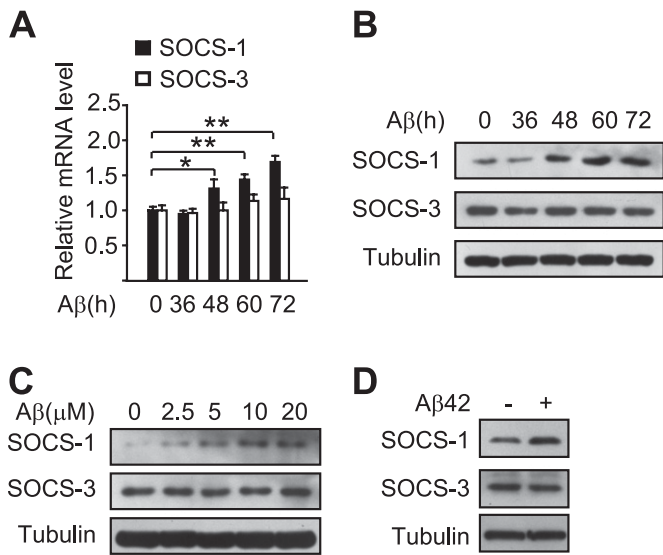
FIG. 4. Aβ induces the upregulation of SOCS-1 in cultured hepatocytes. *A:* Quantitative RT-PCR analysis of SOCS-1 and SOCS-3 mRNA levels in mouse primary hepatocytes treated with 10 μmol/L Aβ25–35 for the indicated times. *B:* Immunoblot analysis of SOCS-1 and SOCS-3 protein levels in mouse primary hepatocytes treated with 10 μmol/L Aβ25–35 for the indicated times. *C:* Immunoblot analysis of SOCS-1 and SOCS-3 protein levels in mouse primary hepatocytes treated with the indicated concentrations of Aβ25–35 for 60 h. *D:* Immunoblot analysis of SOCS-1 and SOCS-3 protein levels in mouse primary hepatocytes treated with 10 μmol/L Aβ42 for 60 h. Data are presented as mean and SEM. *P < 0.05, **P < 0.01.

Obesity is associated with an increased risk of developing insulin resistance and type 2 diabetes (43). In humans, plasma Aβ has a positive correlation with increased body fat (17). APP is overexpressed in subcutaneous abdominal adipocytes from obese humans (16). ApoE4 genotype, a high genetic risk factor for AD, has defects in Aβ clearance (5). Male obese ApoE4 carriers presented increased blood insulin and glucose levels (44). High-fat/cholesterol diet can promote Aβ generation in mice (42,45). These findings raised the possibility that Aβ may contribute to the complicated metabolic syndrome caused by obesity. In addition, APP23 transgenic AD model mice crossed with *ob/ob* or NSY diabetic model mice showed a deteriorated diabetic phenotype (4). Mice loss of β-site amyloid precursor protein-cleaving enzyme 1 exhibited reduced Aβ level and improved peripheral insulin sensitivity (46). These reports support the negative effect of Aβ on insulin sensitivity. We observed that Aβ-induced insulin resistance was not obvious in cultured hepatocytes until treatment for 48 h, and then the impaired insulin signaling lasted and deteriorated with time (Fig. 2D and Supplementary Fig. 2B). Similarly, the impaired glucose tolerance and insulin tolerance also worsened with time in APP/PS1 mice (Fig. 1C–H). These results are consistent with the chronic pathogenesis of T2DM and AD.

Previous studies showed that the physiological levels of plasma Aβ40/42 may range from tens to hundreds of picograms per milliliter (17,38), which are consistent with our observation (Fig. 1A and Supplementary Table 1). Aβ is prone to aggregate both in vitro and in vivo (47), and Aβ deposition is detectable in tissues other than brain in AD patients (48). However, whether Aβ deposition is detectable in the periphery of hyperglycemic subjects needs to be studied in the future. The Aβ used in this study was preincubated at 37°C. This method has been reported to promote the aggregation of Aβ (49). Immunoblot showed that the preincubation of Aβ resulted in various Aβ forms from monomers to oligomers and higher order forms (Supplementary Fig. 5). Which form of Aβ plays the major
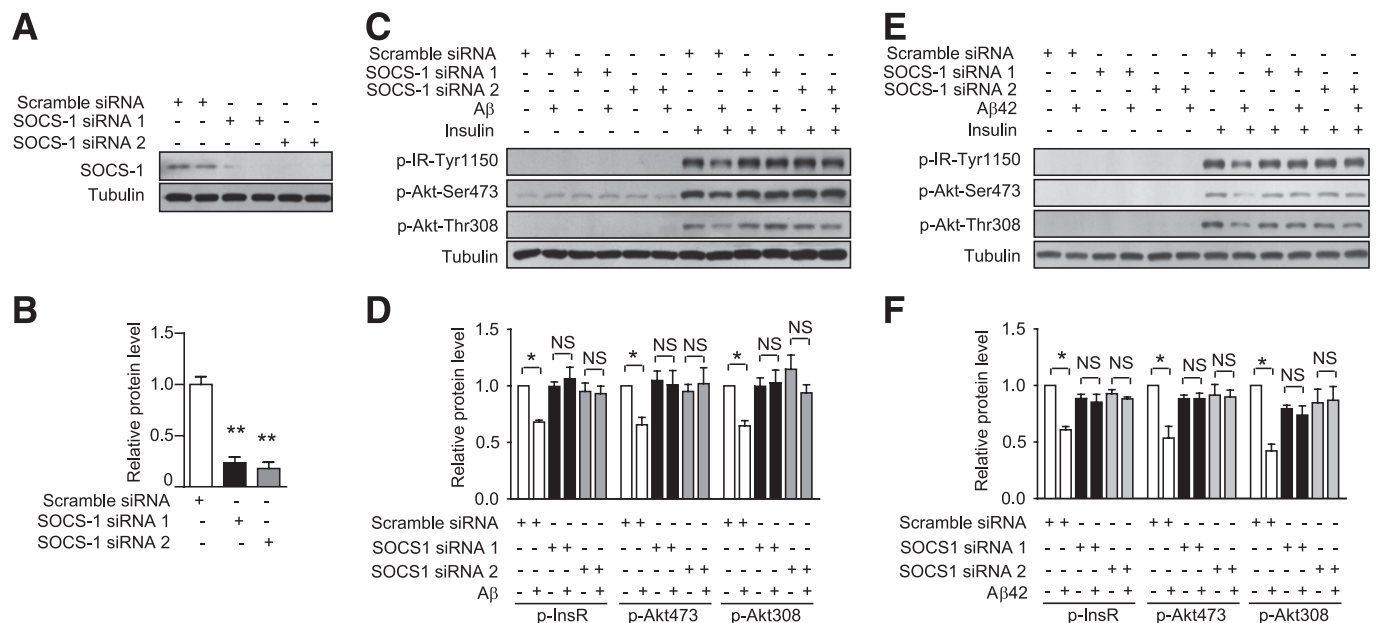

FIG. 5. Upregulation of SOCS-1 is required for the insulin resistance induced by Aβ. *A:* Knockdown of SOCS-1 in primary hepatocytes by two different siRNAs was confirmed by immunoblot. *B:* Quantification of SOCS-1 protein levels in *A. C:* Phosphorylation states of InsR and Akt in primary hepatocytes treated with or without Aβ25–35 for 60 h in the presence of the indicated siRNA with or without 100 nmol/L insulin for 20 min were analyzed by immunoblot. *D:* Quantification of phosphorylated InsR and Akt levels in *C. E:* Phosphorylation states of InsR and Akt in primary hepatocytes treated with or without Aβ42 for 60 h in the presence of the indicated siRNA with or without 100 nmol/L insulin for 20 min were analyzed by immunoblot. *F:* Quantification of phosphorylated InsR and Akt levels in *E.* All the protein levels were normalized to tubulin. Data are presented as mean and SEM. *P < 0.05, **P < 0.01. NS, no significant difference.
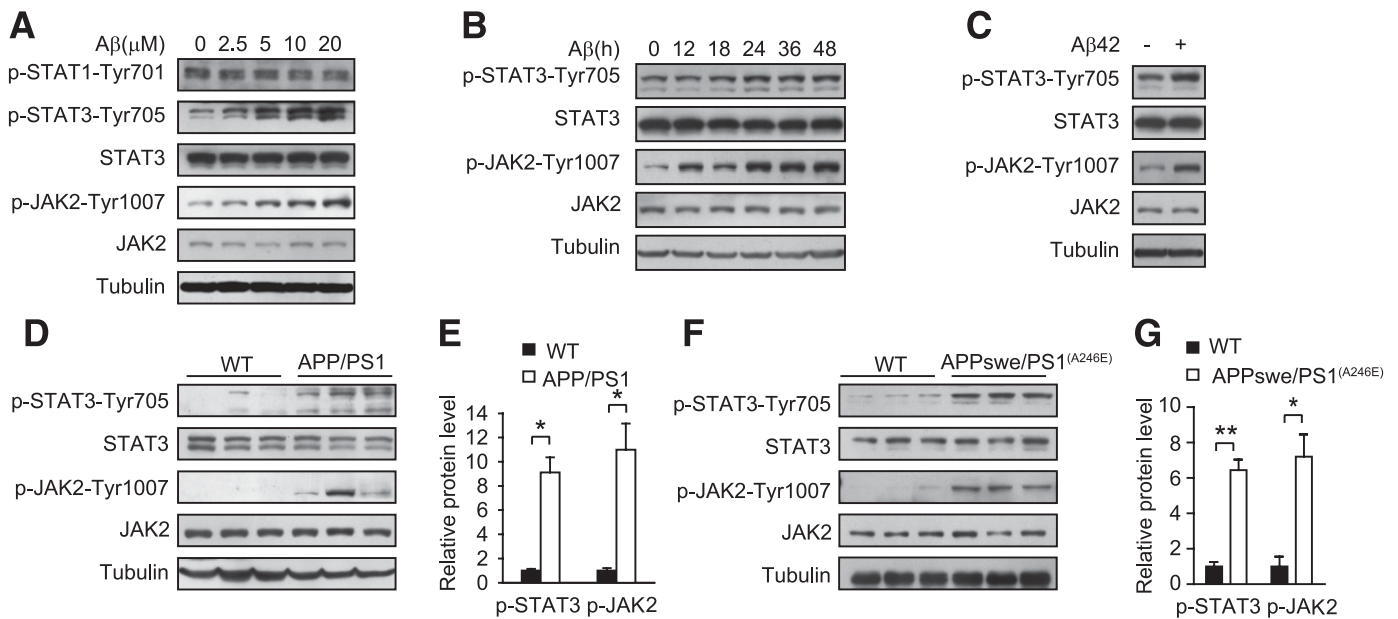
FIG. 6. Aβ induces the activation of JAK2/STAT3. *A*: Immunoblot analysis of phosphorylation levels of STAT1, STAT3, and JAK2 in mouse primary hepatocytes treated with the indicated concentrations of Aβ25–35 for 36 h. *B*: Immunoblot analysis of phosphorylation levels of STAT3 and JAK2 in mouse primary hepatocytes treated with 10 μmol/L Aβ25–35 for the indicated times. *C*: Immunoblot analysis of phosphorylation levels of STAT3 and JAK2 in mouse primary hepatocytes treated with 10 μmol/L Aβ42 for 36 h. *D*: Immunoblot analysis of liver STAT3 and JAK2 phosphorylation states in APP/PS1 mice and wild-type (WT) littermates at 20 weeks of age ($n = 3$ per genotype). *E*: Quantification of phosphorylated STAT3 and JAK2 levels in *D*. *F*: Immunoblot analysis of liver STAT3 and JAK2 phosphorylation states in APPswe/PS1[(A246E)] mice and WT controls at 9 months of age. *G*: Quantification of phosphorylated STAT3 and JAK2 levels in *F*. All the protein levels were normalized to tubulin. Data are presented as mean and SEM. *$P < 0.05$, **$P < 0.01$.

role in Aβ-induced impaired hepatic insulin signaling is yet to be investigated in the future.

It has been reported that cytokines induce insulin resistance by induction of several SOCS proteins (34). In this study, we showed that Aβ specifically upregulated SOCS-1 but didn't affect SOCS-3 protein levels in hepatocytes (Fig. 4*B*–*D*) and mouse liver (Fig. 3*B* and *C*), which implicate that the upregulation of SOCS-1 by Aβ does not result from the induction of inflammatory cytokines. Consistently, we didn't observe obvious inflammatory reaction in liver,
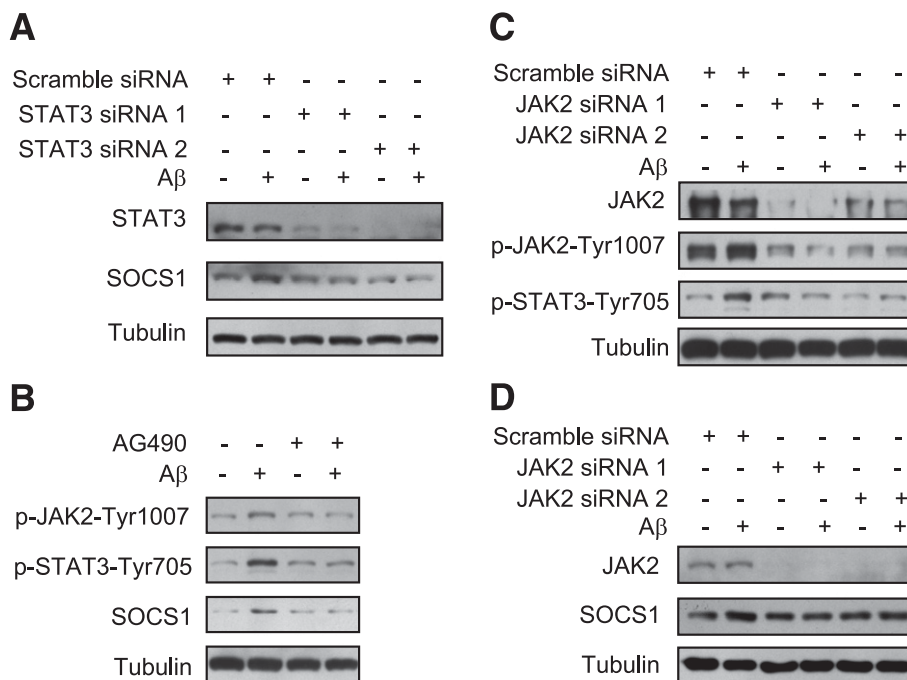

FIG. 7. JAK2/STAT3 signaling is required for the SOCS-1 upregulation induced by Aβ. *A*: Knockdown of STAT3 by siRNA blocked the upregulation of SOCS-1 by Aβ. *B*: Inhibition of JAK2 by AG490 blocked the phosphorylation of JAK2 and STAT3 and the upregulation of SOCS-1 induced by Aβ. *C*: Knockdown of JAK2 by siRNA blocked the phosphorylation of JAK2 and STAT3 induced by Aβ. *D*: Knockdown of JAK2 by siRNA blocked the upregulation of SOCS-1 induced by Aβ.

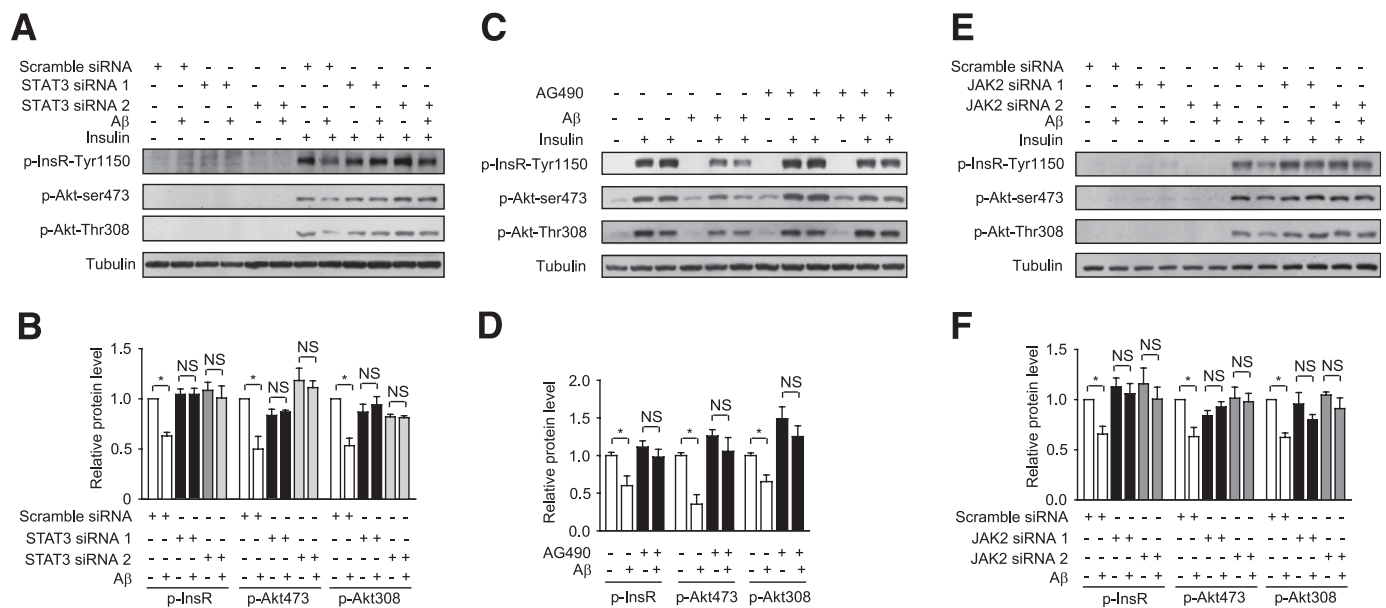FIG. 8. JAK2/STAT3 signaling is required for the insulin resistance induced by Aβ. *A*: Knockdown of STAT3 by siRNA enhanced insulin-stimulated phosphorylation of InsR and Akt under insulin-resistant conditions induced by Aβ. *B*: Quantification of phosphorylated InsR and Akt levels shown in *A*. *C*: Inhibition of JAK2 by AG490 enhanced insulin-stimulated phosphorylation of InsR and Akt under insulin-resistant conditions induced by Aβ. *D*: Quantification of phosphorylated InsR and Akt levels shown in *C*. *E*: Knockdown of JAK2 by siRNA enhanced insulin-stimulated phosphorylation of InsR and Akt under insulin-resistant conditions induced by Aβ. *F*: Quantification of phosphorylated InsR and Akt levels shown in *E*. All the protein levels were normalized to tubulin. Data are presented as mean and SEM. *$P < 0.05$. NS, no significant difference.

muscle, and WAT of APP/PS1 mice (Supplementary Fig. 4*B–D*). SOCS-1 is increased in the liver of insulin-resistant obese animals (35,50). Similarly, we observed that SOCS-1 is upregulated in the liver of APP/PS1 mice (Fig. 3*A–C*). SOCS-1 directly overexpressed in the liver can cause insulin resistance, and inhibition of SOCS-1 in obese diabetic mice improves insulin sensitivity (35). In addition, reduction of SOCS-1 in 3T3-L1 adipocytes alleviates the impaired insulin signaling caused by TNF-α (50). Consistently, we found APP/PS1 mice with upregulation of SOCS-1 in liver is insulin resistant (Fig. 1*C–I*), and knockdown of SOCS-1 in hepatocytes can attenuate the insulin resistance induced by Aβ (Fig. 5*C–F*). It has been reported that overexpression of SOCS-1 can target IRS1 and IRS2 for ubiquitin-mediated degradation in HEK293 cells (51). Another study reported SOCS-1 can bind to the InsR and inhibit its signaling transduction, whereas it didn't affect IRS protein levels (50). In our study, immunoblot showed that hepatic IRS1 and IRS2 protein levels were similar between APP/PS1 mice and littermate controls (Supplementary Fig. 6*A* and *B*). Primary hepatocytes treated with Aβ42 or SOCS-1 siRNA also showed similar IRS1 and IRS2 protein levels (Supplementary Fig. 6*C* and *D*), and the purity and viability of primary hepatocytes were confirmed and shown in Supplementary Fig. 7. The underlying mechanism for how Aβ-induced SOCS-1 attenuates insulin signaling needs to be further investigated.

It has been reported that cytokines upregulate SOCS proteins via activation JAK/STAT signaling (34). In this study, we observed that Aβ upregulates SOCS-1 through JAK2/STAT3 pathway to induce insulin resistance (Figs. 7 and 8). In hepatocytes, Aβ activated JAK2/STAT3 after treatment for about 24 h (Fig. 6*B*), and then upregulated SOCS-1 and impaired insulin signaling after treatment for about 48 h (Figs. 2*D* and 4*B*). It was reported that glucosamine requires 18-h treatment to impair insulin signaling in hepatocytes (23), and the development of insulin resistance in mice fed

high-fat diet needs more than 2 months (23). Thus it is reasonable to observe the development of insulin resistance in heptocytes after a chronic treatment. It has been reported that Aβ is an inducer of reactive oxygen species (ROS) (6). On the other hand, ROS have been shown to induce the activation of JAK2 (52). So ROS might be involved in the activation of JAK2/STAT3 signaling by Aβ. Future studies to figure out the upstream signaling of JAK2/STAT3 in Aβ-induced insulin resistance will be important to further elucidate the underlying molecular mechanisms.

Insulin signaling is involved in a variety of neuronal functions (12). Meanwhile, previous in vitro and in vivo studies showed insulin increases the extracellular level of Aβ by promoting its production/secretion and inhibiting its degradation via insulin-degrading enzyme (11,12). In addition, in the central nervous system, Aβ has been reported to compromise insulin signaling to impair neuronal function (7–10). Aβ competitively binds to InsR, interferes with its autophosphorylation, and prevents the activation of downstream kinases required for long-term potentiation in hippocampal neurons (7,10). Aβ oligomers caused downregulation of plasma membrane InsR and synaptic spine deterioration in hippocampal neurons, which can be prevented by insulin in a rosiglitazone-enhanceable manner (8,9). These studies suggest that the early neuronal damage in AD might be triggered by Aβ-induced impairment of insulin signaling, and stimulation of insulin signaling is a potential strategy to treat AD (53). Whether binding to InsR and downregulation of plasma membrane InsR are involved in Aβ-induced insulin resistance in peripheral tissues needs to be further studied. Our study focused on the role of Aβ in the periphery and demonstrates that Aβ induces insulin resistance in hepatocytes by activating the JAK2/STAT3/SOCS-1 signaling pathway. These findings suggest that strategies aimed at reducing peripheral Aβ signaling might be beneficial for insulin resistance and T2DM.

ACKNOWLEDGMENTS

REFERENCES

1. Stumvoll M, Goldstein BJ, van Haeften TW. Type 2 diabetes: principles of pathogenesis and therapy. Lancet 2005;365:1333–1346
2. Janson J, Laedtke T, Parisi JE, O'Brien P, Petersen RC, Butler PC. Increased risk of type 2 diabetes in Alzheimer disease. Diabetes 2004;53:474–481
3. Craft S, Zallen G, Baker LD. Glucose and memory in mild senile dementia of the Alzheimer type. J Clin Exp Neuropsychol 1992;14:253–267
4. Takeda S, Sato N, Uchio-Yamada K, et al. Diabetes-accelerated memory dysfunction via cerebrovascular inflammation and Abeta deposition in an Alzheimer mouse model with diabetes. Proc Natl Acad Sci USA 2010;107:7036–7041
5. Citron M. Alzheimer's disease: strategies for disease modification. Nat Rev Drug Discov 2010;9:387–398
6. Querfurth HW, LaFerla FM. Alzheimer's disease. N Engl J Med 2010;362:329–344
7. Townsend M, Mehta T, Selkoe DJ. Soluble Abeta inhibits specific signal transduction cascades common to the insulin receptor pathway. J Biol Chem 2007;282:33305–33312
8. Zhao WQ, De Felice FG, Fernandez S, et al. Amyloid beta oligomers induce impairment of neuronal insulin receptors. FASEB J 2008;22:246–260
9. De Felice FG, Vieira MN, Bomfim TR, et al. Protection of synapses against Alzheimer's-linked toxins: insulin signaling prevents the pathogenic binding of Abeta oligomers. Proc Natl Acad Sci USA 2009;106:1971–1976
10. Xie L, Helmerhorst E, Taddei K, Plewright B, Van Bronswijk W, Martins R. Alzheimer's beta-amyloid peptides compete for insulin binding to the insulin receptor. J Neurosci 2002;22:RC221
11. Qiu WQ, Folstein MF. Insulin, insulin-degrading enzyme and amyloid-beta peptide in Alzheimer's disease: review and hypothesis. Neurobiol Aging 2006;27:190–198
12. Takeda S, Sato N, Rakugi H, Morishita R. Molecular mechanisms linking diabetes mellitus and Alzheimer disease: beta-amyloid peptide, insulin signaling, and neuronal function. Mol Biosyst 2011;7:1822–1827
13. DeMattos RB, Bales KR, Parsadanian M, et al. Plaque-associated disruption of CSF and plasma amyloid-beta (Abeta) equilibrium in a mouse model of Alzheimer's disease. J Neurochem 2002;81:229–236
14. Deane R, Du Yan S, Submamaryan RK, et al. RAGE mediates amyloid-beta peptide transport across the blood-brain barrier and accumulation in brain. Nat Med 2003;9:907–913
15. Roher AE, Esh CL, Kokjohn TA, et al. Amyloid beta peptides in human plasma and tissues and their significance for Alzheimer's disease. Alzheimers Dement 2009;5:18–29
16. Lee YH, Tharp WG, Maple RL, Nair S, Permana PA, Pratley RE. Amyloid precursor protein expression is upregulated in adipocytes in obesity. Obesity (Silver Spring) 2008;16:1493–1500
17. Balakrishnan K, Verdile G, Mehta PD, et al. Plasma Abeta42 correlates positively with increased body fat in healthy individuals. J Alzheimers Dis 2005;8:269–282
18. Lee YH, Martin JM, Maple RL, Tharp WG, Pratley RE. Plasma amyloid-beta peptide levels correlate with adipocyte amyloid precursor protein gene expression in obese individuals. Neuroendocrinology 2009;90:383–390
19. Coraci IS, Husemann J, Berman JW, et al. CD36, a class B scavenger receptor, is expressed on microglia in Alzheimer's disease brains and can mediate production of reactive oxygen species in response to beta-amyloid fibrils. Am J Pathol 2002;160:101–112
20. El Khoury J, Hickman SE, Thomas CA, Cao L, Silverstein SC, Loike JD. Scavenger receptor-mediated adhesion of microglia to beta-amyloid fibrils. Nature 1996;382:716–719
21. Valdes CT, Elkind-Hirsch KE. Intravenous glucose tolerance test-derived insulin sensitivity changes during the menstrual cycle. J Clin Endocrinol Metab 1991;72:642–646
22. Wang Q, Jiang L, Wang J, et al. Abrogation of hepatic ATP-citrate lyase protects against fatty liver and ameliorates hyperglycemia in leptin receptor-deficient mice. Hepatology 2009;49:1166–1175
23. Sun C, Zhang F, Ge X, et al. SIRT1 improves insulin sensitivity under insulin-resistant conditions by repressing PTP1B. Cell Metab 2007;6:307–319
24. Yang Q, Graham TE, Mody N, et al. Serum retinol binding protein 4 contributes to insulin resistance in obesity and type 2 diabetes. Nature 2005;436:356–362
25. Wang K, Wang C, Xiao F, Wang H, Wu Z. JAK2/STAT2/STAT3 are required for myogenic differentiation. J Biol Chem 2008;283:34029–34036
26. Wan J, Fu AK, Ip FC, et al. Tyk2/STAT3 signaling mediates beta-amyloid-induced neuronal cell death: implications in Alzheimer's disease. J Neurosci 2010;30:6873–6881
27. Kim I, Lee J, Hong HJ, et al. A relationship between Alzheimer's disease and type 2 diabetes mellitus through the measurement of serum amyloid-beta autoantibodies. J Alzheimers Dis 2010;19:1371–1376
28. Jankowsky JL, Fadale DJ, Anderson J, et al. Mutant presenilins specifically elevate the levels of the 42 residue beta-amyloid peptide in vivo: evidence for augmentation of a 42-specific gamma secretase. Hum Mol Genet 2004;13:159–170
29. Burgess BL, McIsaac SA, Naus KE, et al. Elevated plasma triglyceride levels precede amyloid deposition in Alzheimer's disease mouse models with abundant A beta in plasma. Neurobiol Dis 2006;24:114–127
30. Ghiso J, Shayo M, Calero M, et al. Systemic catabolism of Alzheimer's Abeta40 and Abeta42. J Biol Chem 2004;279:45897–45908
31. Pike CJ, Walencewicz-Wasserman AJ, Kosmoski J, Cribbs DH, Glabe CG, Cotman CW. Structure-activity analyses of beta-amyloid peptides: contributions of the beta 25-35 region to aggregation and neurotoxicity. J Neurochem 1995;64:253–265
32. Wyss-Coray T, Mucke L. Inflammation in neurodegenerative disease—a double-edged sword. Neuron 2002;35:419–432
33. Hotamisligil GS. Inflammation and metabolic disorders. Nature 2006;444:860–867
34. Rønn SG, Billestrup N, Mandrup-Poulsen T. Diabetes and suppressors of cytokine signaling proteins. Diabetes 2007;56:541–548
35. Ueki K, Kondo T, Tseng YH, Kahn CR. Central role of suppressors of cytokine signaling proteins in hepatic steatosis, insulin resistance, and the metabolic syndrome in the mouse. Proc Natl Acad Sci USA 2004;101:10422–10427
36. Liu L, Herukka SK, Minkeviciene R, van Groen T, Tanila H. Longitudinal observation on CSF Abeta42 levels in young to middle-aged amyloid precursor protein/presenilin-1 doubly transgenic mice. Neurobiol Dis 2004;17:516–523
37. Chiba T, Yamada M, Sasabe J, et al. Amyloid-beta causes memory impairment by disturbing the JAK2/STAT3 axis in hippocampal neurons. Mol Psychiatry 2009;14:206–222
38. Assini A, Cammarata S, Vitali A, et al. Plasma levels of amyloid beta-protein 42 are increased in women with mild cognitive impairment. Neurology 2004;63:828–831
39. Fukumoto H, Tennis M, Locascio JJ, Hyman BT, Growdon JH, Irizarry MC. Age but not diagnosis is the main predictor of plasma amyloid beta-protein levels. Arch Neurol 2003;60:958–964
40. Sims-Robinson C, Kim B, Rosko A, Feldman EL. How does diabetes accelerate Alzheimer disease pathology? Nat Rev Neurol 2010;6:551–559
41. Cao D, Lu H, Lewis TL, Li L. Intake of sucrose-sweetened water induces insulin resistance and exacerbates memory deficits and amyloidosis in a transgenic mouse model of Alzheimer disease. J Biol Chem 2007;282:36275–36282
42. Ho L, Qin W, Pompl PN, et al. Diet-induced insulin resistance promotes amyloidosis in a transgenic mouse model of Alzheimer's disease. FASEB J 2004;18:902–904

43. Kahn SE, Hull RL, Utzschneider KM. Mechanisms linking obesity to insulin resistance and type 2 diabetes. Nature 2006;444:840–846
44. Kypreos KE, Karagiannides I, Fotiadou EH, et al. Mechanisms of obesity and related pathologies: role of apolipoprotein E in the development of obesity. FEBS J 2009;276:5720–5728
45. Thirumangalakudi L, Prakasam A, Zhang R, et al. High cholesterol-induced neuroinflammation and amyloid precursor protein processing correlate with loss of working memory in mice. J Neurochem 2008;106:475–485
46. Meakin PJ, Harper AJ, Hamilton DL, et al. Reduction in BACE1 decreases body weight, protects against diet-induced obesity and enhances insulin sensitivity in mice. Biochem J 2012;441:285–296
47. Chen YR, Glabe CG. Distinct early folding and aggregation properties of Alzheimer amyloid-beta peptides Abeta40 and Abeta42: stable trimer or tetramer formation by Abeta42. J Biol Chem 2006;281:24414–24422
48. Joachim CL, Mori H, Selkoe DJ. Amyloid beta-protein deposition in tissues other than brain in Alzheimer's disease. Nature 1989;341:226–230
49. Mason RP, Jacob RF, Walter MF, et al. Distribution and fluidizing action of soluble and aggregated amyloid beta-peptide in rat synaptic plasma membranes. J Biol Chem 1999;274:18801–18807
50. Ueki K, Kondo T, Kahn CR. Suppressor of cytokine signaling 1 (SOCS-1) and SOCS-3 cause insulin resistance through inhibition of tyrosine phosphorylation of insulin receptor substrate proteins by discrete mechanisms. Mol Cell Biol 2004;24:5434–5446
51. Rui L, Yuan M, Frantz D, Shoelson S, White MF. SOCS-1 and SOCS-3 block insulin signaling by ubiquitin-mediated degradation of IRS1 and IRS2. J Biol Chem 2002;277:42394–42398
52. Shimizu S, Hiroi T, Ishii M, et al. Hydrogen peroxide stimulates tetrahydrobiopterin synthesis through activation of the Jak2 tyrosine kinase pathway in vascular endothelial cells. Int J Biochem Cell Biol 2008;40:755–765
53. Liao FF, Xu H. Insulin signaling in sporadic Alzheimer's disease. Sci Signal 2009;2:pe36